

Mechanically probing the folding pathway of single RNA molecules

Ulrich Gerland*, Ralf Bundschuh†, and Terence Hwa*

**Department of Physics, University of California at San Diego, La Jolla, California 92093-0319 and*

†*Department of Physics, The Ohio State University, 174 W 18th Av., Columbus, Ohio 43210-1106*

(Dated: February 7, 2020)

We study theoretically the denaturation of single RNA molecules by mechanical stretching, focusing on signatures of the (un)folding pathway in molecular fluctuations. Our model describes the interactions between nucleotides by incorporating the experimentally determined free energy rules for RNA secondary structure, while exterior single stranded regions are modeled as freely jointed chains. For exemplary RNA sequences (hairpins and the *Tetrahymena thermophila* group I intron), we compute the quasi-equilibrium fluctuations in the end-to-end distance as the molecule is unfolded by pulling on opposite ends. Unlike the average quasi-equilibrium force-extension curves, these fluctuations reveal clear signatures from the unfolding of individual structural elements. We find that the resolution of these signatures depends on the spring constant of the force-measuring device, with an optimal value intermediate between very rigid and very soft. We compare and relate our results to recent experiments by Liphardt *et al.* [*Science* 292, 733-737 (2001)].

The advent and refinement of techniques to apply and measure forces on single molecules has allowed remarkable experiments probing the elastic properties and structural transitions of biomolecules such as DNA (see, e.g., Bockelmann *et al.*, 1998; Maier *et al.*, 2000; Smith *et al.*, 1996) and proteins (see, e.g., Rief *et al.*, 1997). Recently, single-molecule experiments using optical tweezers were also performed to study the unfolding of small RNA molecules under an applied force (Liphardt *et al.*, 2001, 2002). RNA molecules, besides functioning as messengers of sequence information in the process of protein synthesis, also have many biological functions that intricately depend on a precisely folded RNA structure, e.g., as ribosomal RNA or as self-splicing introns (Cech, 1993). The formation of RNA structure (‘RNA folding’) is therefore an important biophysical process, which however is currently not understood in sufficient detail (Tinoco and Bustamante, 1999). Pulling experiments (Liphardt *et al.*, 2001, 2002), possibly in combination with single-molecule fluorescence methods (Zhuang *et al.*, 2000, 2002), promise to reveal important aspects of RNA structure, its folding pathways and kinetics, and eventually its biological function.

The experiment of Liphardt *et al.* (2001) has shown that pulling on simple structural units of RNA, e.g., a single hairpin, yields characteristic features in the force-extension curve (FEC), which can be used to deduce the unfolding free energy and the size of the structural element. Moreover, the observation of end-to-end distance time-traces at constant force revealed that the unfolding and refolding of these simple structures proceeds directly without intermediates, and the opening/closing rates could be extracted from the time-traces. From the theoretical side, it is interesting to ask how far, in principle, the pulling approach could be pushed to study larger RNA molecules and how the resolution of such approaches depends on parameters of the experimental setup. Here, we expand our previous model for RNA pulling experiments (Gerland *et al.*, 2001), and address

these questions. The model incorporates the experimentally known free energy rules for RNA secondary structure (Walter *et al.*, 1994) and a polymer model for the elastic properties of single-stranded RNA (ssRNA), but neglects pseudoknots and tertiary interactions, the energetics of which are currently poorly characterized.

Our model yields predictions for force-extension measurements, including fluctuations, and the mechanical (un)folding pathway for any given RNA sequence. Below, we begin with the P5ab hairpin used by Liphardt *et al.* (2001) and demonstrate that our model yields an FEC which is in semi-quantitative agreement with the experimental curve. This agreement gives us confidence that our model is sufficiently realistic to permit its use to explore general questions regarding sequence-dependent signatures in mechanical single-molecule experiments on RNA.

We first address the question of intermediates in the unfolding pathway and show that, according to our model, a small modification in the sequence of the P5ab hairpin can change its two-state folding behavior and introduce a locally dominant intermediate. However, whether this intermediate state can be observed through quasi-equilibrium fluctuation measurements critically depends on the experimental conditions: If the force-measuring device is a “soft spring”, the hairpin unfolds without any visible intermediates. Only when the force is measured with a stiff spring, an intermediate state can be observed.

We then consider a larger RNA molecule, the group I intron of *Tetrahymena thermophila* with a sequence of about 400 bases and a known secondary structure containing many individual elements (Cech, 1993). Previous theoretical work predicted that equilibrium FEC’s of large RNA’s are smooth and display no secondary structure dependent features, due to a compensation effect between individual structural elements (Gerland *et al.*, 2001). Here, we find that even in the absence of structure-based features in the FEC, measurements of

the equilibrium fluctuations of the entire molecule can still be used to obtain information on the (un)folding pathway. Also, for this longer molecule a good choice of the stiffness of the force-measuring device is important for the determination of the pathway.

Model

We consider an experimental setup where the two ends of an RNA molecule are attached to a force- and extension-measuring device, e.g. an atomic force microscope or beads trapped by optical tweezers. [For the sake of concreteness, we consider the optical tweezer setup as an example here, see Fig. 1(a).] In an idealized theoretical model, the RNA molecule (in essence, a highly nonlinear elastic element for the present context) is connected in series with a linear harmonic spring, and the total extension is externally controlled, see Fig. 1(b). The linear spring models the force-measuring device. E.g., for optical tweezers, its harmonic potential approximates the potential of the optical trap, and the spring constant λ is adjustable in the experiment through the laser intensity. The extension of the spring, R_s , corresponds to the position of the bead with respect to the minimum of the trapping potential, and is measured as a function of the total extension R_t . The average force acting on the RNA molecule and its average extension are

$$\langle f \rangle = \lambda \langle R_s \rangle, \quad (1)$$

$$\langle R \rangle = R_t - \langle R_s \rangle. \quad (2)$$

Here, $\langle \dots \rangle$ denotes a thermal average over all accessible conformations of the RNA molecule and the spring at fixed total extension R_t . Throughout this article, we assume that the pulling experiment is performed slowly enough, such that the RNA molecule can fully sample its conformational space on timescales which are short compared to the external timescale of the imposed stretching process. The average $\langle \dots \rangle$ then includes an average over all possible secondary structures of the molecule.

Partition function. To calculate the averages in Eqs. (1) and (2), as well as the averages of other observables to be introduced below, we first determine the partition function, $Z(R_t)$, of the RNA molecule and the spring at fixed total extension R_t . In previous work (Gerland et al., 2001), we computed the partition function of the RNA molecule alone in the *fixed distance ensemble*. Here, we explicitly take the force-measuring spring into account; varying the spring constant λ interpolates between the fixed distance ensemble for stiff springs (large λ) and the fixed force ensemble for soft springs (small λ). Intermediate spring constants effectively put the RNA molecule into a *mixed ensemble*. The explicit consideration of the spring in the model is necessary here, not only for a closer modeling of the actual experimental setup, but also from a theoretical point of view, since the force *fluctuations* diverge in the fixed distance ensemble and our aim is to study fluctuation measurements.

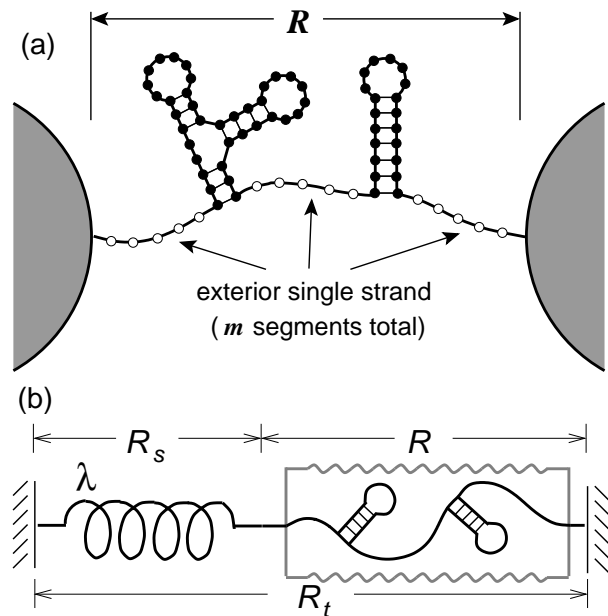


FIG. 1 Sketch of the system considered here. (a) In a typical experimental setup, the two ends of an RNA molecule are attached to beads the position of which is controlled, e.g., with optical tweezers. (b) In a theoretical model, the potential of the optical trap can be approximated by a linear spring (with spring constant λ). This spring is connected in series with a highly nonlinear elastic element (the RNA molecule, usually with an additional linker). The total extension, R_t , is externally controlled, while the individual extensions, R_s and R , undergo thermal fluctuations.

A model for an experimental setup such as the one sketched in Fig. 1(a) requires two separate parts, one that contains only information on the free energies for the secondary structures of the RNA sequence, and another which describes the polymer properties of ssRNA (Gerland et al., 2001). The coupling between these two parts is through the total length of the *exterior* ssRNA segments of the molecule, i.e. the number m of bases that actually “feel” the applied force, see Fig. 1(a). For every fixed total extension R_t , the system has to find a compromise between lowering the RNA binding energy by *decreasing* m , and gaining entropy (plus lowering elastic energy) by *increasing* m . The secondary structure part is given by the partition function, $Q(m)$, summed over all secondary structures of the RNA molecule with a fixed number m of exterior single-stranded bases¹. The polymer properties of ssRNA then enter through a function $W_{\text{tot}}(R_t; m)$, which denotes the *total* end-to-end distance distribution of a ssRNA molecule of m bases in series with the spring². The total partition function, $Z(R_t)$ is

¹ We account for the width of stems within the exterior single strand by increasing the base count m by three for each stem.

² For simplicity, we restrict the spring to be collinear with the end-to-end distance of the RNA molecule.

then simply the convolution of $\mathcal{Q}(m)$ with $W_{\text{tot}}(R_t; m)$,

$$Z(R_t) = \sum_m \mathcal{Q}(m) W_{\text{tot}}(R_t; m). \quad (3)$$

The detailed calculation of $\mathcal{Q}(m)$ is described in (Gerland et al., 2001). Briefly, the calculation takes the experimentally determined rules for the binding free energies of RNA secondary structures (Walter et al., 1994) into account, but neglects tertiary structure effects and pseudoknots. Our method is based on a recursive method to calculate the partition function (McCaskill, 1990) as implemented in the ‘Vienna RNA package’ (Hofacker et al., 1994), but introduces an additional recursion relation for the calculation of $\mathcal{Q}(m)$.

The total end-to-end distance distribution of a ssRNA molecule of m bases in series with the spring can be expressed as

$$W_{\text{tot}}(R_t; m) = \int_0^\infty dR W_{\text{RNA}}(R; m) \frac{e^{-\beta\lambda(R_t-R)^2/2}}{\sqrt{2\pi/\beta\lambda}}, \quad (4)$$

where $W_{\text{RNA}}(R; m)$ denotes the distribution of the ssRNA molecule alone. We model the ssRNA as an elastic freely jointed chain, i.e., as a chain of segments with unrestricted relative orientations, whereas the segment length r is constrained by a harmonic potential $V(r) = \kappa(r-b)^2/2$. The average segment length b corresponds to the Kuhn length of a non-interacting ssRNA chain. The number of segments of the elastic freely jointed chain used to represent an RNA molecule with m bases is chosen as ml/b where l is the base to base distance of ssRNA. This yields $W_{\text{RNA}}(R; m) \approx C \frac{h}{2\pi R} [q(h)]^{ml/b} e^{-hR}$, where C is a normalization constant, $q(h) = \langle e^{-h\mathbf{z}\cdot\mathbf{r}} \rangle$, and h is determined from $R = \frac{mb}{l} \frac{\partial}{\partial h} \log q(h)$ (Gerland et al., 2001). Such a model has been shown to describe the elastic properties of ssDNA molecules (Maier et al., 2000; Montanari and Mézard, 2001). Since we are not aware of the corresponding data for RNA, we use the DNA values for the polymer parameters as obtained by Montanari and Mézard (2001) through fitting to the experiment of Maier et al. (2000), i.e. $l=0.7\text{nm}$, $b=1.9\text{nm}$, and $(\kappa/k_B T)^{-1/2} = 0.1\text{nm}$ (we do not expect a large difference in the single strand properties of DNA and RNA, because of the high similarity between their chemical structures). We take the free energy parameters for RNA secondary structure as supplied with the Vienna package (version 1.3.1) at room temperature $T = 25^\circ\text{C}$. The salt concentrations at which the free energy parameters were measured are $[\text{Na}^+] = 1\text{M}$ and $[\text{Mg}^{++}] = 0\text{M}$.

Observables. From the partition function (3) we get the total free energy $F(R_t) = -k_B T \log Z(R_t)$, the average force $\langle f \rangle = \partial F(R_t)/\partial R_t$, and through Eqs. (1) and (2) also the average extension $\langle R \rangle$ of the RNA molecule. The equilibrium fluctuations in the extension of the RNA molecule are given by $\text{var}(R) = \langle R^2 \rangle - \langle R \rangle^2 = [\lambda - \partial^2 F/\partial R_t^2]/\beta\lambda^2$. Using these relations, one can

show³ that the variance is related to the derivative of the force-extension curve as measured *in the mixed ensemble* through

$$\text{var}(R) = \frac{k_B T}{\lambda + \partial\langle f \rangle/\partial\langle R \rangle}, \quad (5)$$

which holds exactly and is of the general fluctuation-dissipation theorem form.

To study the unfolding pathway, we introduce the weight $x_m(R_t)$ for the secondary structures with m exterior open bases at a given value of R_t ,

$$x_m(R_t) = \frac{\mathcal{Q}(m) W_{\text{tot}}(R_t; m)}{Z(R_t)}, \quad (6)$$

which satisfy the normalization condition $\sum_m x_m = 1$. The binding probability of base i and j at given R_t may then be expressed as

$$P_{ij}(R_t) = \sum_m x_m(R_t) p_{ij}(m), \quad (7)$$

where $p_{ij}(m)$ denotes the base pairing probability in the ensemble of structures with fixed m , which can be calculated as described previously (Gerland et al., 2001).

Results

We first consider the P5ab hairpin, which is the simplest RNA molecule studied in the experiment of Liphardt et al. (2001), and is of a size that typically occurs as a structural subunit in larger RNA molecules. Fig. 2(a) shows its native structure and the experimental FEC for P5ab with added linker taken from Liphardt et al. (2001). Fig. 2(b) shows the FEC that results from our model⁴, both for a relatively stiff spring with $\lambda = 0.2$ pN/nm and a relatively soft spring of $\lambda = 0.01$ pN/nm. [Here, we modeled the linker, which in the experiment connects the RNA molecule to the beads, simply as a chain of non-binding bases at the end of the RNA sequence. The length of this chain (326 bases) is our only fitting parameter.] The experimental and the theoretical curves compare relatively well. In particular, both curves show a characteristic ‘‘hump’’ at a force close to 14 pN, which identifies the opening of the hairpin. The experimental curve displays a slight drop of the

³ The derivation is straightforward after observing that

$$\frac{\partial\langle f \rangle}{\partial\langle R \rangle} = \frac{\partial\langle f \rangle}{\partial R_t} / \frac{\partial\langle R \rangle}{\partial R_t} = \frac{\partial^2 F(R_t)/\partial R_t^2}{1 - (1/\lambda)\partial^2 F(R_t)/\partial R_t^2}.$$

⁴ The native structure of P5ab contains two non-standard G–A base pairs for which no quantitative information on the binding energies is available. We therefore follow the suggestion of Ref. (Liphardt et al., 2001) and approximate the binding energy of G–A basepairs by replacing them with G–U pairs.

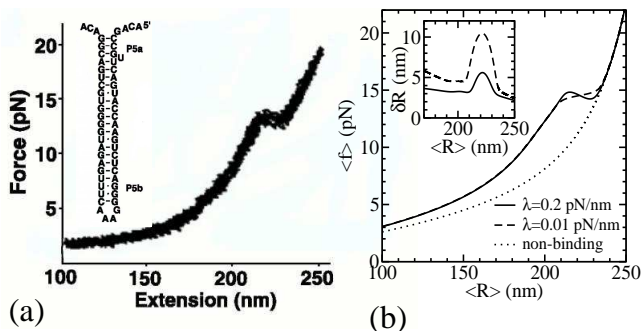


FIG. 2 Force-extension curve (FEC) for the P5ab hairpin with added linker. (a) Native structure of the hairpin and its FEC as experimentally determined by Liphardt et al. (2001). (b) FEC for P5ab as results from our model for two different spring constants λ (solid and dashed line; see main text for details). The dotted line represents the FEC for a non-binding sequence of the same length as P5ab. Inset: End-to-end distance fluctuations as a function of the average extension.

force within the hump similar to the theoretical curve for the stiff spring. This is consistent with the fact that the optical trap of the experiment has a rather stiff spring constant of about 0.1 pN/nm (Liphardt et al., 2001). The force drop occurs as the hairpin opens, because the released single-strand creates “slack” in the polymer.

These FEC’s contain useful information: The area between the FEC of P5ab and the FEC for a non-binding sequence of the same length (dotted line) gives the total binding free energy of the hairpin, and the number of bases in the hairpin can be read off by fitting a curve such as the dotted line to the lower part of the FEC (see also the discussion by Liphardt et al., 2001). Note that as long as the experiment is performed in quasi-equilibrium, the area under the FEC is independent of the spring constant, and therefore the same in the fixed-force and the fixed-distance ensemble. Loosely speaking, the FEC in the fixed-force ensemble could therefore be considered as the ‘Maxwell construction’ of the FEC in the fixed-distance ensemble.

It is clear from Fig. 2 that our model of the linker is not quantitatively correct, since the experimental FEC starts out flatter and then becomes steeper than the theoretical curve. To achieve a better quantitative agreement with the experimental FEC, the polymer properties of the linkers, the salt dependence of the base pairing energies, and the base pairing energies of the G–A base pairs would have to be taken into account properly. However, the semi-quantitative agreement we have achieved seems sufficient to justify the use of our model as a tool to study the general questions outlined in the introduction.

We begin by characterizing the unfolding process of the P5ab hairpin within our model. In the experiment of Liphardt et al. (2001), the time traces of the end-to-end extension at fixed forces around 14 pN show the characteristic pattern of a bistable system, i.e. the unfolding proceeds directly, without intermediates. To cal-

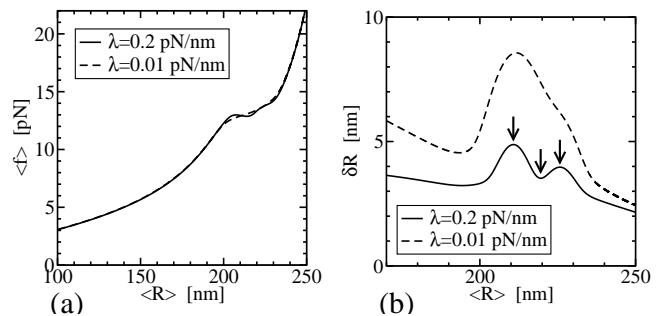


FIG. 3 Calculated force-extension characteristics for the modified P5ab hairpin (G–A basepairs replaced by U–U) for a hard ($\lambda = 0.2$ pN/nm) and a soft ($\lambda = 0.01$ pN/nm) harmonic potential of the optical tweezer. (a) The average FEC, which resembles very much the FEC in Fig. 2(b). (b) The fluctuations of the extension as a function of the average extension. While the curve is very similar to the inset of Fig. 2(b) for a soft spring, it develops a pronounced minimum corresponding to an intermediate state for a hard spring. The arrows indicate the positions at which the x_m -distributions shown in Fig. 4 were calculated.

culate theoretical time traces would require a full kinetic treatment of the RNA folding/unfolding process which is beyond the scope of the present article. Instead, we determine the time-average of the fluctuations in the end-to-end extension as a function of the mean force or extension. Note that while *in theory*, the FEC and the fluctuations are directly related through Eq. (5), these two quantities are *measured independently*. Since the fluctuations can be measured with much greater accuracy than the derivative of the FEC, they can be used as a complementary source of information.

The inset of Fig. 2(b) shows the root-mean-square fluctuations in the extension, $\delta R = \sqrt{\text{var}(R)}$, as a function of the average extension, $\langle R \rangle$, in the range of extensions over which the hairpin opens. Consistent with the two state behavior found experimentally, we observe a single peak of the fluctuations at the extension (or equivalently force) at which the transition takes place. Physically, this peak is caused by continual kinetic fluctuations between the open and the closed state of the hairpin.

Hairpin with intermediate. Next, we address the question whether the simple two-state behavior observed for P5ab is a generic property for hairpins of this typical size. The discussion of this question also serves as a preparation for our ensuing study of a larger RNA with more complicated structure. To this end, we modify the sequence of the P5ab hairpin slightly by replacing the two G–A basepairs with U’s on both strands, which leads to a small interior loop in the hairpin. This change does not significantly affect the FEC, see Fig. 3(a), however the fluctuations δR take on a qualitatively different behavior, as shown in Fig. 3(b): For a soft spring, the δR -curve shows only a single peak as before, but a stiff spring yields two maxima with a pronounced minimum in between. At this minimum, the configurational dis-

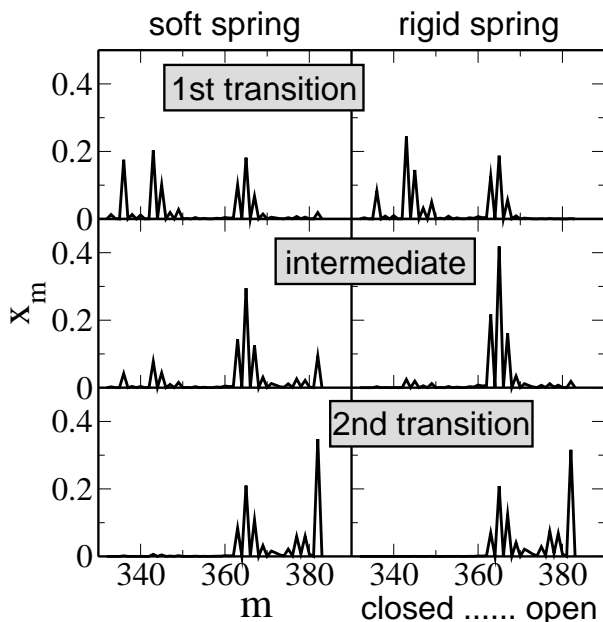


FIG. 4 Probability distributions in m -space for the modified P5ab hairpin. The left column is calculated with a soft spring ($\lambda = 0.01$ pN/nm), and the right column with a stiff spring ($\lambda = 0.2$ pN/nm). The curves in the top/middle/bottom row are calculated for different average extensions $\langle R \rangle$ corresponding to the positions indicated by the arrows in Fig. 3(b) [first peak, minimum, and second peak in the fluctuation curve, respectively]. For the stiff spring, the distribution at the minimum is almost entirely localized on the intermediate state. In contrast, the distribution is spread out over all three states for the soft spring at the same average extension.

tribution of the molecule is localized on an intermediate state, which strongly reduces the fluctuations in the extension. This is demonstrated explicitly in Fig. 4, which shows the probability distribution in m -space, i.e. x_m as given by Eq. (6) (see caption for details).

The stiffness of the external spring therefore limits the attainable resolution of the measurements: At low resolution the hairpin appears as a two-state folder, while an intermediate state appears at higher resolution. This observation is in line with the comment of Fernandez et al. (2001) who discuss the experiment of Liphardt et al. (2001) by analogy to patch clamp experiments, where an intermediate state in the opening of an ion channel appears only at high resolution. While an increase in the spring constant increases the resolution, it decreases the amplitude of the fluctuations, which renders them harder to detect. For the present purpose, the optimal value for λ results from a tradeoff between low resolution and low amplitude. Clearly, increasing λ can increase the resolution only up to the point where the floppiness of the RNA plus linker becomes resolution limiting (this point corresponds approximately to $\lambda = 0.1$ pN/nm for the hairpin sequences discussed above). This point marks the optimal choice for λ , unless the spacial resolution of the experimental apparatus is restrictive already at

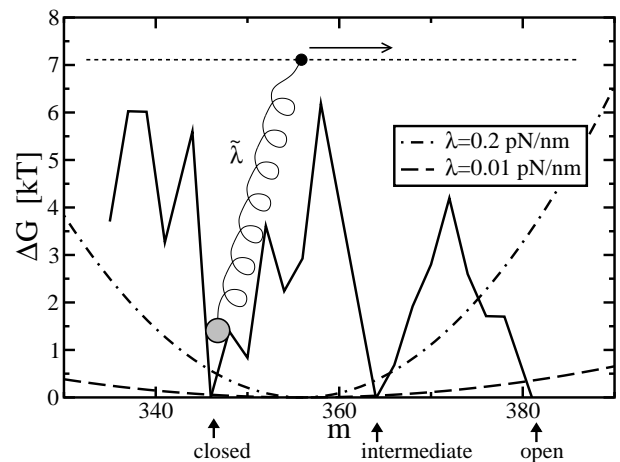


FIG. 5 Particle with an attached spring in the free energy landscape of the modified P5ab hairpin. The other end position of the spring is externally controlled (see Gerland et al., 2001, for the details of the mapping to the RNA unzipping problem). The spring in this picture represents the measurement device, the linker, and the ssRNA and has an effective spring constant $\tilde{\lambda}$. Its harmonic potential for $\lambda = 0.01$ pN/nm and $\lambda = 0.2$ pN/nm is shown as the dashed and dash-dotted lines, respectively. With the soft spring, the particle can jump from the closed to the open state immediately as soon as the force is strong enough to overcome the energy barrier. The hard spring has a steeper harmonic potential and thus the particle will first jump into the intermediate state and later into the open state as the end of the spring is moved towards larger m .

smaller values of λ . The role of the spring constant in dynamic force spectroscopy measurements is discussed by Heymann and Grubmüller (2000).

Intuitively, the fact that the appearance of the intermediate state depends on the spring constant is best understood by mapping the unzipping problem onto the problem of a particle with an attached spring in a random potential and coupled to a thermal bath (see Fig. 5). As the other end of the spring is moved in one direction, the particle performs a ‘stick-slip’ motion (Bockelmann et al., 1998). With a stiff spring, the particle hops over short distances and tends to be localized, while the particle can make long jumps, sliding over many valleys, when the spring is soft.

RNA molecule with multiple structural sub-units. We now proceed to an RNA molecule with a more complex secondary structure. What could fluctuation measurements teach us in such a case? Can we apply the insight gained above to study the (un)folding pathway? One might ask whether the mechanical (un)folding pathway is well-defined at all for a more complex molecule, e.g. could the order in which different states are visited depend on parameters such as the spring constant λ ? The answer to the latter question is no: The number of exterior unpaired bases, m , is a natural and well-defined reaction coordinate, and on average the distribution x_m will always shift to larger m when R_t is increased. Hence,

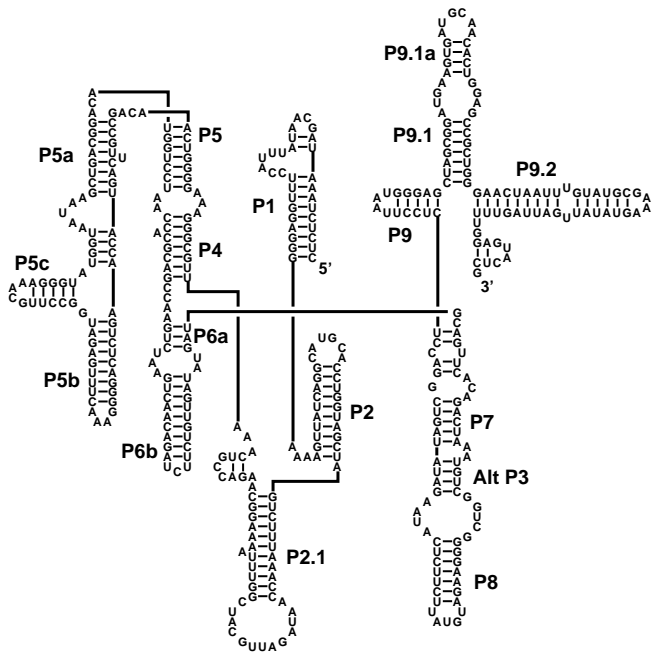


FIG. 6 Secondary structure of the *Tetrahymena thermophila* group I intron as obtained from the Vienna package. The overall structure, and almost all individual basepairs, are identical to the one of the inactive conformation as determined in Ref. (Pan and Woodson, 1998) (we follow the labeling introduced there).

λ can only affect the resolution of individual states in m -space, but not the average order in which they are visited. By definition, in quasi-equilibrium, the average unfolding pathway is identical with the average (re)folding pathway. Hence the mechanical (un)folding pathway is well-defined.

The self-splicing intron from *Tetrahymena thermophila* is a convenient example for an RNA molecule with a structure of moderate complexity. Its sequence (Genbank # J01235) contains 419 bases and its known structure consists of 19 structural elements labeled P1, P2, P2.1, P3, etc. It was the first RNA molecule to be shown to have a catalytic activity and has since been studied in great detail (Cech, 1993). Its active, i.e. self-splicing, conformation contains a pseudoknot, which is essential for the function. However, it also has a known and well characterized inactive conformation without pseudoknot (Pan and Woodson, 1998; Zhuang et al., 2000). The minimum free energy structure obtained from the Vienna RNA Package (which supplies the basis to our model) is shown in Fig. 6. The overall structure, and almost all individual basepairs, are identical to the one of the inactive conformation as determined by Pan and Woodson (1998) (we follow the labeling introduced there), which confirms that the RNA free energy rules describe the nucleotide interactions quite well.

As expected (Gerland et al., 2001), the equilibrium FEC in Fig. 7(a) shows no signatures of the secondary structure, due to ‘compensation’ between different struc-

tural elements, and therefore does not allow the reconstruction of the unfolding pathway for a known structure, let alone the determination of an unknown secondary structure. Two better ways to probe the mechanical (un)folding pathway are: (i) An analysis of end-to-end distance time traces in equilibrium, as performed by Liphardt et al. (2001) for the P5ab hairpin, and (ii) an analysis of nonequilibrium FEC’s, as recently done in the Berkeley group (S. Dumont & I. Tinoco Jr., private communication). Without a proper model for RNA kinetics

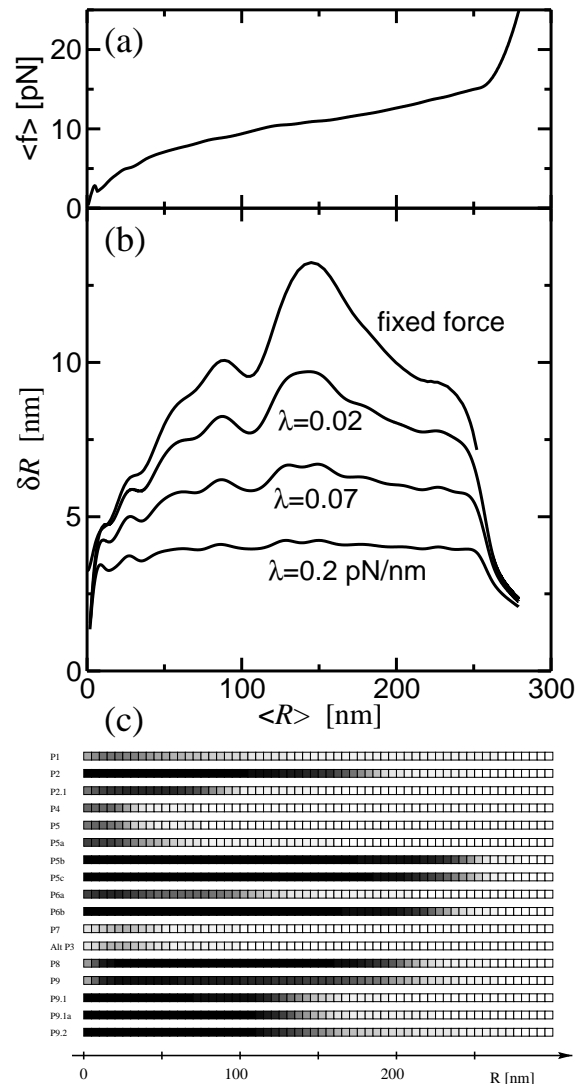


FIG. 7 Calculated force-extension characteristics of the *Tetrahymena thermophila* group I intron. (a) FEC. (b) Fluctuations in the extension of the ribozyme for different stiffness λ of the force measuring device. (c) Fractional opening for all of the structural elements at $\lambda = 0.02$ pN/nm. A black square indicates that the structural element is completely intact while a white square indicates that all base pairs of the element have been opened. It can be seen that the FEC lacks all structural features. In contrast, the fluctuations display pronounced peaks that coincide with the disappearance of specific structural elements.

at hand, we will consider here only the former.

As for the P5ab hairpin above, we compute the equilibrium fluctuations δR , which correspond to the root-mean-square average of the experimental time traces $R(t)$. Obviously, our averaged δR contains less information than experimental $R(t)$ traces. Nevertheless, as Fig. 7(b) shows, already the equilibrium fluctuations δR display interesting sequence-dependent features, i.e. local maxima and minima. Again, the minima can be interpreted as intermediate states along the (un)folding pathway, and the maxima as structural transitions. [Note that the central peak close to $\langle R \rangle = 150$ nm splits into two peaks as the stiffness of the spring is increased, indicating the appearance of a new intermediate on the (un)folding pathway.] We conclude that while the FEC loses its features as the structure of the molecule becomes more complex the analysis of equilibrium fluctuations presented above for the P5ab hairpin can still be applied to extract information on the (un)folding pathway of more complex molecules. Specifically, the ability to resolve intermediate states still depends on the stiffness of the force-measuring device that has to be chosen according to a trade-off between resolution of intermediate structures and absolute measurable size of the fluctuations.

Within our theoretical model it is a simple matter to identify the structural transitions associated with the peaks. For each of the structural elements labeled in Fig. 6, the normalized sum of the base pair probabilities (computed with Eqs. (6–7)) is plotted as a function of the mean extension in Fig. 7(c) for $\lambda = 0.02$ pN/nm. For instance, one can directly read off that the central peak is associated with the parallel opening of P9.1, P9.1a, and P9.2, whereas P5b, P5c open last.

To obtain the same information in the experiment will be more laborious, but should be possible given the known secondary structure, since at every mean extension (or force) only a small number (up to 3) structural elements open in parallel, which would lead to a number of characteristic plateaus in the experimental $R(t)$ traces. The identification of the plateaus with the corresponding elements can be obtained by cutting the molecule at several places between the known secondary structure elements and performing the same measurement on subsequences. [A similar approach was taken for recent nonequilibrium experiments in the Berkeley group (S. Dumont & I. Tinoco Jr., private communication).] Obtaining the mechanical (un)folding pathway for a moderately sized RNA with known secondary structure therefore appears feasible by measuring the equilibrium fluctuations δR .

Summary and Discussion

Single-molecule experiments are particularly useful when the molecule under study can take on several conformations, e.g. folding intermediates, because in these

cases bulk measurements usually yield only average properties, while single-molecule measurements can characterize each of the different conformations. Here, we predicted experimental signatures of such folding intermediates in the quasi-equilibrium fluctuations of the end-to-end distance. We found that a local minimum in the fluctuations curve indicates a locally stable intermediate state in the average mechanical unfolding pathway (which is well-defined and identical to the (re)folding pathway). The number of local minima in the fluctuations curve can therefore serve as a lower estimate of the number of locally stable intermediate states in this pathway. Furthermore, these signatures could be used to reconstruct the (un)folding pathway of an RNA molecule with a known secondary structure by cutting the sequence at appropriate positions and individually probing different substructures of the molecule.

We also showed that the stiffness of the force-measuring device plays a crucial role in determining the resolution of the quasi-equilibrium fluctuations curve. If the device is too soft, some local minima can be lost, while a too rigid device has a low fluctuation amplitude and therefore a low signal-to-noise ratio. The optimal choice for the stiffness (see ‘Results’) leads to the best estimate for the number of locally stable intermediate states along the pathway and increases the degree to which the pathway could be reconstructed with the “cutting approach”. The dependence on the stiffness has a simple intuitive explanation within the statistical mechanics problem of a particle with an attached spring in a one-dimensional energy landscape (see Fig. 5): A stiff force-measuring device corresponds to a rigid spring, which tends to localize the particle in valleys of the landscape (i.e., locally stable intermediates) and forces it to make small jumps as it is pulled along the landscape. On the other hand, a soft spring allows the particle to spread out and make long jumps, effectively hiding the intermediates in the equilibrium curve.

We hope that this view, which also explains the smoothness of quasi-equilibrium FEC’s for large RNA’s (Gerland et al., 2001), will be useful for the design and interpretation of future experiments. Of course, experiments typically record not only the average fluctuations, but the detailed time-traces of the end-to-end distance (Liphardt et al., 2001). These traces probe the kinetics of structural rearrangements in RNA, and could provide even more detailed resolution of intermediate states (if the kinetics is slow enough to be resolvable in the experiment). However, we expect that it is still helpful to make the choice for the stiffness of the force-measuring device as discussed above, in order to limit the number of states that contribute to each of the timetraces.

Although single-molecule experiments on RNA have already produced remarkable results, there are many desirable future developments. For instance, it appears that the current approaches are not well-suited to measure the secondary structure of an unknown molecule (e.g., in the ‘cutting approach’ one would not know where to cut and

it would be too laborious to try all positions). Is there a direct way to mechanically measure the secondary structure? Also, could one detect signatures of pseudoknots or even tertiary interactions? We hope that theoretical models of the type presented here can be useful for the planning and design of new experimental approaches in the future.

Note. After completion of this work, we learned of a related theoretical study by S. Cocco, J.F. Marko, and R. Monasson (preprint, cond-mat/0207609). These authors present a kinetic model for the end-to-end distance fluctuations of stretched RNA molecules, which nicely complements our thermodynamic study.

Acknowledgments. We are grateful to S.M. Block, S. Dumont, H. Isambert, J. Liphardt, D. Lubensky, I. Tinoco, and S.A. Woodson for stimulating discussions. U.G. was supported in part by a German DAAD fellowship. R.B. and T.H. acknowledge support by the NSF through Grant No. DMR-9971456, DBI-9970199, and the Beckmann foundation.

References

- Bockelmann, U., B. Essevaz-Roulet, and F. Heslot. 1998. DNA strand separation studied by single molecule force measurements. *Phys. Rev. E* 58:2386-2394.
- Cech, T.R. 1993. Structure and mechanism of the large catalytic RNAs: group I and group II introns and ribonuclease P. In *The RNA World* (Gesteland, R.F. & Atkins, J.F., eds). 239-269, Cold Spring Harbor Laboratory Press, Plainview, NY.
- Fernandez, J.M., S. Chu, A.F. Oberhauser. 2001. RNA structure: Pulling on Hair(pins). *Science* 292:653-654.
- Gerland, U., R. Bundschuh, and T. Hwa. 2001. Force-induced denaturation of RNA. *Biophys. J.* 81:1324-1332.
- Heymann, B. and H. Grubmüller. 2000. Dynamic Force Spectroscopy of Molecular Adhesion Bonds. *Phys. Rev. Lett.* 84:6126-6129.
- Hofacker, I.L., W. Fontana, P.F. Stadler, S. Bonhoeffer, M. Tacker, and P. Schuster. 1994. Fast folding and comparison of RNA secondary structures. *Monatshefte f. Chemie* 125:167-188.
- Liphardt, J., B. Onoa, S.B. Smith, I. Tinoco, and C. Bustamante. 2001. Reversible Unfolding of Single RNA Molecules by Mechanical Force. *Science* 292:733-737.
- Liphardt, J., S. Dumont, S.B. Smith, I. Tinoco, and C. Bustamante. 2002. Equilibrium information from nonequilibrium measurements in an experimental test of Jarzynski's equality. *Science* 296:1832-1835.
- Maier, B., D. Bensimon, and V. Croquette. 2000. Replication by a single DNA polymerase of a stretched single-stranded DNA. *Proc. Natl. Acad. Sci. USA* 97:12002-12007.
- McCaskill, J.S. 1990. The equilibrium partition function and base pair binding probabilities for RNA secondary structure. *Biopolymers* 29:1105-1119.
- Montanari, A. and M. Mézard. 2001. Hairpin formation and elongation of biomolecules. *Phys. Rev. Lett.* 86:2178-2181.
- Pan, J. and S.A. Woodson. 1998. Folding Intermediates of a Self-splicing RNA: Mispairing of the Catalytic Core. *J. Mol. Biol.* 280:597-609.
- Rief, M., M. Gautel, F. Oesterhelt, J.M. Fernandez, and H.E. Gaub. 1997. Reversible unfolding of individual titin immunoglobulin domains by AFM. *Science* 276:1109-1112.
- Smith, S.B., Y. Cui, and C. Bustamante. 1996. Overstretching B-DNA: the elastic response of individual double-stranded and single-stranded DNA molecules. *Science* 271:795-799.
- Tinoco, I. Jr and C. Bustamante. 1999. How RNA folds. *J. Mol. Biol.* 293:271-281.
- Walter, A.E., D.H. Turner, J. Kim, M.H. Lyttle, P. Muller, D.H. Mathews, and M. Zuker. 1994. Coaxial stacking of helices enhances binding of oligoribonucleotides and improves predictions of RNA folding. *Proc. Natl. Acad. Sci. USA* 91:9218-9222.
- Zhuang, X., L.E. Bartley, H.P. Babcock, R. Russell, T. Ha, D. Herschlag, and S. Chu. 2000. A Single-Molecule Study of RNA Catalysis and Folding. *Science* 288:2048-2051.
- Zhuang, X., H. Kim, M.J.B. Pereira, H.P. Babcock, N.G. Walter, and S. Chu. 2002. Correlating Structural Dynamics and Function in Single Ribozyme Molecules. *Science* 296:1473-1476.